18th International Conference on Structural Mechanics in Reactor Technology (SMiRT 18)
Beijing, China, August 7-12, 2005
SMiRT18-K13-6

FORCED VIBRATION TEST OF AN ABWR NUCLER REACTOR BUILDING – SIMULATION ANALYSIS BY MDOF PARALLEL MODEL

Atsushi ONOUCHI
Manager, Chubu Electric Power Co., Inc., Japan, M.Eng.

Atsushi TACHIBANA*
Senior Staff, Chubu Electric Power Co., Inc., Japan, M.Eng.
1, Toshin-cho, Higashi-ku, Nagoya, 461-8680, Japan
Phone: +81-052-973-3128
Fax: +81-052-973-3173
E-mail:Tachibana.Atsushi@chuden.co.jp

ABSTRACT

The forced vibration test was performed to evaluate the dynamic characteristics of Hamaoka nuclear power plant unit-5 reactor building from May through June in 2003. This report is focusing on the results of the simulation analysis regarding the test and of the seismic response analysis to verify the aseismic design safety under the basic design earthquake motion. First, the simulation analysis is performed to establish an analytical model that can explain the dynamic characteristic similar to the test results. A MDOF(Multi-Degree-Of-Freedom) parallel model is used in the analysis to verify the soil-structure interaction model for design. The simulation results are corresponding well the vibration tests, and it is concluded that the model used in the simulation analysis can well explain the dynamic characteristics of the real nuclear reactor building. Next, the seismic response analysis of this building is carried out in NS and EW direction in order to verify the aseismic design safety under the basic design earthquake motion S1. Comparing the maximum seismic response values under S1 earthquake and the design seismic loads, the former is less than the latter for all members in both directions. Therefore, it is also concluded that the design seismic load and aseismic design safety are verified.

Keywords: Forced vibration test, Simulation analysis, Seismic response analysis, Reactor Building, Multi-Degree-Of-Freedom parallel model,

1. INTRODUCTION

The forced vibration test was performed to evaluate the dynamic characteristics of Hamaoka nuclear power plant unit-5 reactor building from May through June in 2003.Two 10-tonf-type large exciters were used at 5th floor, the fuel-operating floor, for each horizontal excitation in NS and EW directions. Sensors were set up at every 9 floors in order to measure the building responses.

Results of the forced vibration test are shown in the previous paper entitled “Forced vibration test of an ABWR nuclear reactor building –Data analysis and system identification-”. This paper shows the results of the simulation analysis and of the seismic response analysis to verify the aseismic design safety under the basic design earthquake motion. The simulation analysis is performed to establish an analytical model that can explain the dynamic characteristics similar to the test results. A MDOF (Multi-Degree-Of-Freedom) parallel model is used in the analysis to verify the soil-structure interaction model for design. The model for simulation analysis is verified by comparing the analytical results with the test results mainly in resonance curves. In addition, the seismic response analysis of the building is

carried out in NS and EW direction in order to verify the aseismic design safety under the basic design earthquake motion S1.

Sections of the reactor building(R/B), the turbine building(T/B) and the auxiliary building(Ax/B) are shown in Fig.1. A plan of the operating floor (5F) of the R/B is shown in Fig.2.

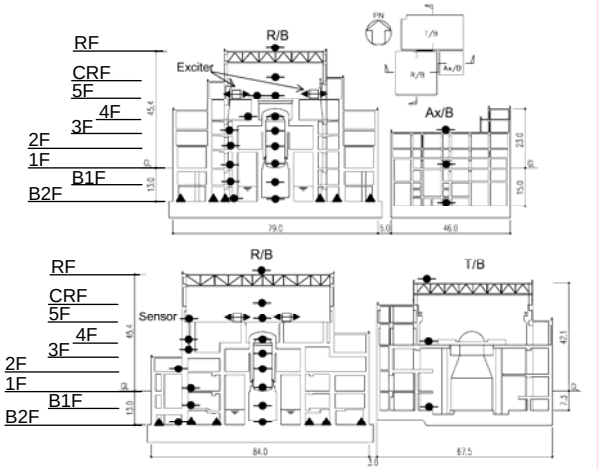

Figure 1 Section through R/B,T/B and Ax/B and instrumentation

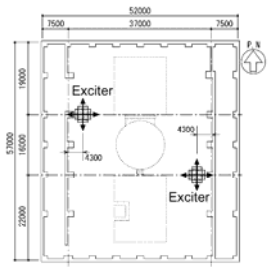

Figure 2 Plan of the operating floor with location of exciter

2. SIMULATION ANALYSIS

2.1 BUILDING MODEL

The model for representing the building considers earthquake-resistant walls consist of outer box walls (OW), inner box walls (IW) and a RCCV wall (RCCV) as a multi-axes lumped-mass model. Columns on the operating floor are also modeled as a multi-axes lumped-mass model with the out-of-plane vibration of IW. Not only earthquake-resistant walls but also main partition walls are considered for stiffness of each beam element in multi axes. Each floor and a roof truss are evaluated as an equivalent shear spring connecting each axis. Weight of each mass reflects the situation at the test date. Thus, There are no water in the fuel pool and suppression pool. Real weight of the building according to progress of the construction is also considered. Properties of concrete are shown in Table 1 that is obtained from material tests using the concrete specimens sampled from the building. Damping ratio h of the building is estimated to be 0.05, while that of the steel roof truss is 0.02.

Table 1 Properties of Concrete

Young's Modulus Ed	4.19×10^{7} kN/m^2
Shear Modulus Gd	1.75×10^{7} kN/m^2

2.2 SOIL MODEL

The model for representing the soil consists of four-axes lumped-mass model that is called MDOF (Multi-Degree-Of-Freedom) parallel model. Each mass for soil is connected horizontally with an axial spring and vertically with a shear spring. Dimensions of the soil model are about 4 times of the building width in horizontal direction and also up to 100m deep. Thickness of the soil model is the same as the width of the building foundation (82m in NS and 87m in EW).

For the boundary condition, viscous boundaries at the bottom, on the side and also in the depth dimension are applied to consider energy dissipating effects. A rotational spring by the rocking of the building foundation is derived from the vibration admittance theory based on three-dimensional wave propagation equation.

To evaluate the frictional effects by the rotational restraint between the soil and the building in the small amplitude of vibration at the test, a rotational spring based on Novak's method is applied on the side of the building. Properties of the backfill soil in NS direction are evaluated from MMR (Man Made Rock) that is located between R/B and T/B from the level below T/B foundation to the level below R/B foundation.

The degradation of the elastic stiffness of the soil is not taken into account due to the small amplitude of vibration at the test. The other properties of the soil and the backfill soil are assumed to be the same as the design value.

Properties of the soil are shown in Table 2. Properties of the backfill soil in the NS/EW sections are also shown in Table 3 and 4. In addition, the soil-building analytical models in the NS/EW directions are shown in Fig.3 and Fig.4.

Table 2 Properties of Soil

Level GL m	Density γ (kN/m^3)	Poisson's ratio ν	Shear Velocity Vs（m/s）	Shear Stiffness Go(10^{3}kN/m^2)	Young's Modulus E(10^{3}kN/m^2)	Damping ratio (%)
0						
-7	20	0.45	240	116	335	5.0
-14	20	0.44	600	721	2076	5.0
-22	20	0.43	680	926	2648	5.0
-40	20	0.42	740	1096	3114	5.0
-70	20	0.41	790	1249	3524	5.0
-100	20	0.40	830	1379	3861	5.0
	21	0.39	910	1741	4840	5.0

Table 3 Properties of Backfill Soil (in NS section)

Properties of Backfill Soil (Shear spring in the NS simulation analysis)

Level (GL m)	Type	Density γ （ kN/m^3）	Poisson's ratio ν	Shear Stiffness Go (? 0^{3}kN/m^2)	Stifness degradation rate G/Go	Shear Stiffness G (? 0^{3}kN/m^2)	Damping ratio (%)
0.0							
-2.0	Backfill Soil	20	0.45	36	1.0	36	5.0
-4.5	Backfill Soil	20	0.45	62	1.0	62	5.0
-7.0	Backfill Soil	20	0.45	79	1.0	79	5.0
-10.0	Backfill Soil	20	0.45	95	1.0	95	5.0
-11.2	Backfill Soil	20	0.45	105	1.0	105	5.0
-13.0	MMR	23	0.17	12000	1.0	12000	5.0
-19.5	MMR	23	0.167	12000	1.0	12000	5.0

Properties of Backfill Soil (Axial spring in the NS simulation analysis)

Level (GL m)	Type	Density γ （ kN/m3）	Poisson's ratio ν	Shear Stiffness Go (? 0^{3}kN/m^2)	Stifness degradation rate G/Go	Young扭 Modulus E (? 0^{3}kN/m^2)	Damping ratio (%)
0.0							
-1.0	Backfill Soil	20	0.45	26	1.0	76	5.0
-3.25	Backfill Soil	20	0.45	51	1.0	148	5.0
-5.75	Backfill Soil	20	0.45	72	1.0	208	5.0
-8.5	Backfill Soil	20	0.45	88	1.0	256	5.0
-11.2	Backfill Soil	20	0.45	102	1.0	296	5.0
-11.5	MMR	23	0.167	12000	1.0	27900	5.0
-13.0	MMR	23	0.167	12000	1.0	27900	5.0
-16.3	MMR	23	0.167	12000	1.0	27900	5.0
-19.50	MMR	23	0.167	12000	1.0	27900	5.0

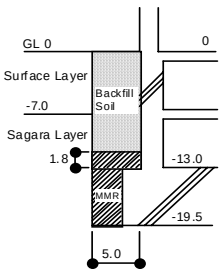

MMR:Man Made Rock

Table 4 Properties of Backfill Soil (in EW section)

Properties of Backfill Soil (Shear spring in the EW simulation analysis)

Level (GL m)	Type	Density γ (kN/m^3)	Poisson's ratio ν	Shear Stiffness Go (? 0^{3}kN/m^2)	Stifness degradation rate G/Go	Shear Stiffness G (? 0^{3}kN/m^2)	Damping ratio (%)
0.0							
-2.0	Backfill Soil	20	0.45	36	1.0	36	5.0
-4.5	Backfill Soil	20	0.45	62	1.0	62	5.0
-7.0	Backfill Soil	20	0.45	79	1.0	79	5.0
-10.0	Backfill Soil	20	0.45	95	1.0	95	5.0
-13.0	Backfill Soil	20	0.45	109	1.0	109	5.0

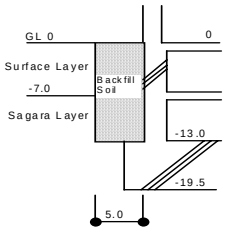

Properties of Backfill Soil (Axial spring in the EW simulation analysis)

Level (GL m)	Type	Density γ (kN/m^3)	Poisson's ratio ν	Shear Stiffness Go (? 0^{3}kN/m^2)	Stifness degradation rate G/Go	Young扭 Modulus E (? 0^{3}kN/m^2)	Damping ratio (%)
0.0							
-1.0	Backfill Soil	20	0.45	26	1.0	76	5.0
-3.25	Backfill Soil	20	0.45	51	1.0	148	5.0
-5.75	Backfill Soil	20	0.45	72	1.0	208	5.0
-8.5	Backfill Soil	20	0.45	88	1.0	256	5.0
-11.5	Backfill Soil	20	0.45	103	1.0	299	5.0
-13.0	Backfill Soil	20	0.45	113	1.0	328	5.0

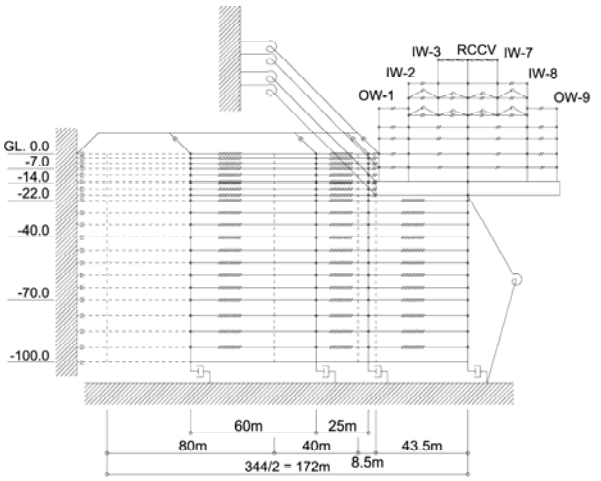

Figure 3 Simulation analysis model (NS direction)

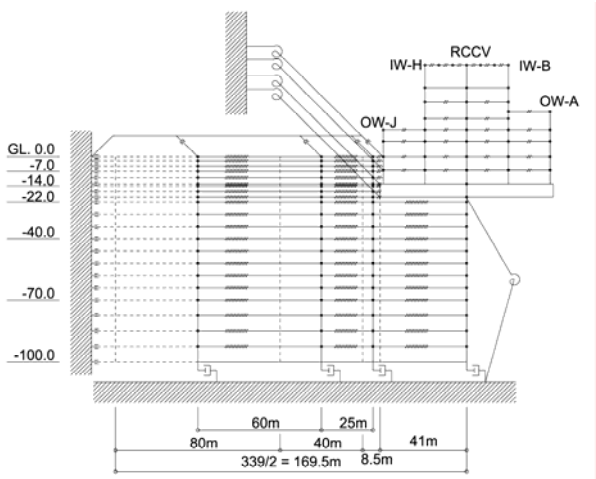

Figure 4 Simulation analysis model (EW direction)

2.3 SIMULATION ANALYSIS RESULT

Comparisons of resonance and phase curves between analytical and test results are shown in Fig.5 to Fig.8. For the resonance curves in the direction of NS shown in Figure 5 and 6, there is a small difference on the first peak's frequency around 4Hz between analytical and test results. Also, the amplitude of the first peak around 4Hz of analytical results is larger than that of test results. For around 9Hz peak excited the roof truss and around 9Hz valley observed below the crane floor (CRF) that may be caused by energy absorbing effect, the tendency of analytical results is corresponding well to that of test results. From the viewpoint of the difference between NS and EW, analytical results are corresponding well to the test results such that the amplitude of the first peak around 4Hz in EW is larger than that in NS.

Comparisons of first vibration mode for inner box between analytical and test results are shown in Fig.9 and Fig.10. Table 5 shows the ratio of first vibration mode's displacement at rooftop level by sway, rocking and elastic deformation of members. The first peak's frequency of the test result in the direction of NS is 4.1Hz and that of the analytical result is 3.4Hz. The first peak's frequency of the test result in the direction of EW is 4.4Hz and that of the analytical result is 4.1Hz. Since the ratio of sway and rocking of the analytical result is corresponding well to that of the test result in the direction of EW, the first peak's frequency of the analytical result is corresponding well to that of the test result. On the other hand, since the ratio of sway of the analytical result is larger than that of test result in the direction of NS, there is a small difference on the first peak's frequency between analytical and test results. That might be due to the influence on the turbine building in the north side of the reactor building.

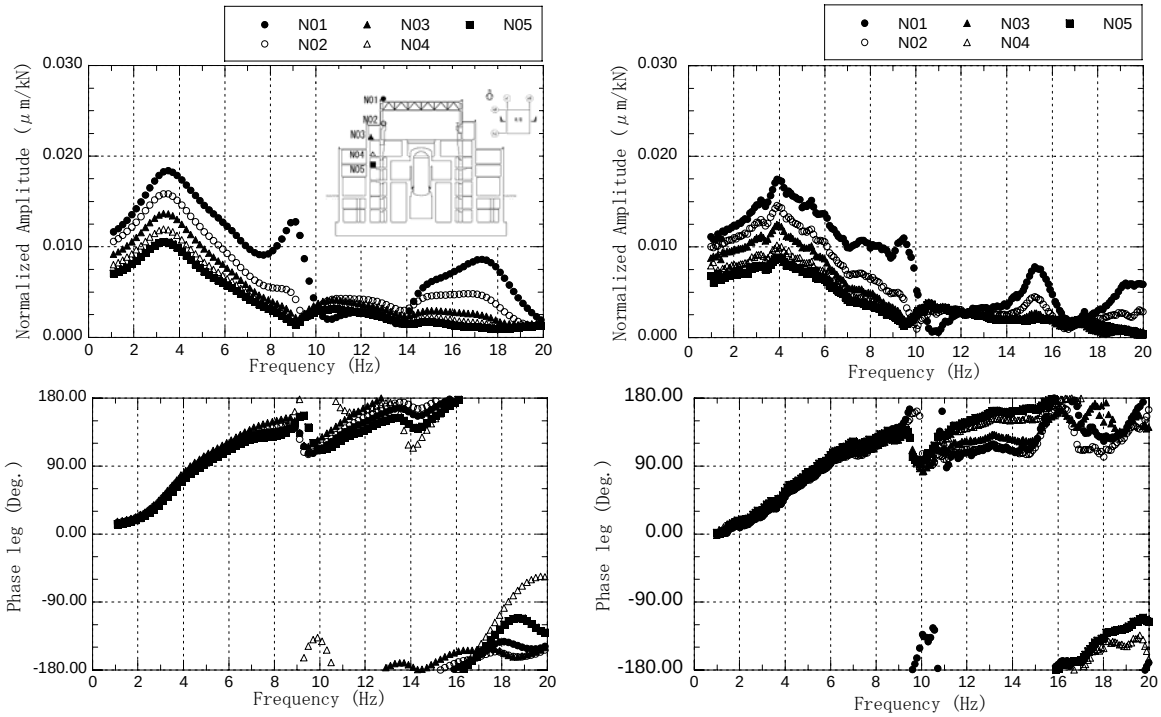

Analytical Test

Figure 5 Comparison of Simulation and Test (NS direction;RF-3F)

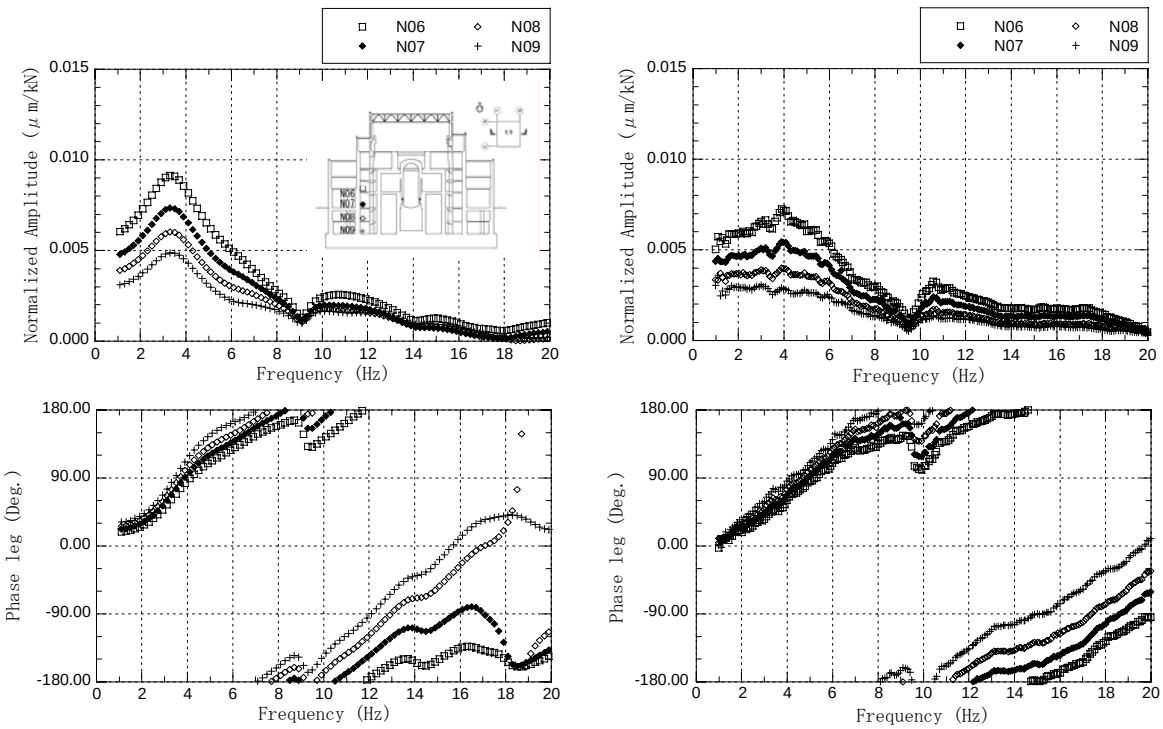

Analytical Test

Figure 6 Comparison of Simulation and Test (NS direction;2F-B2F)

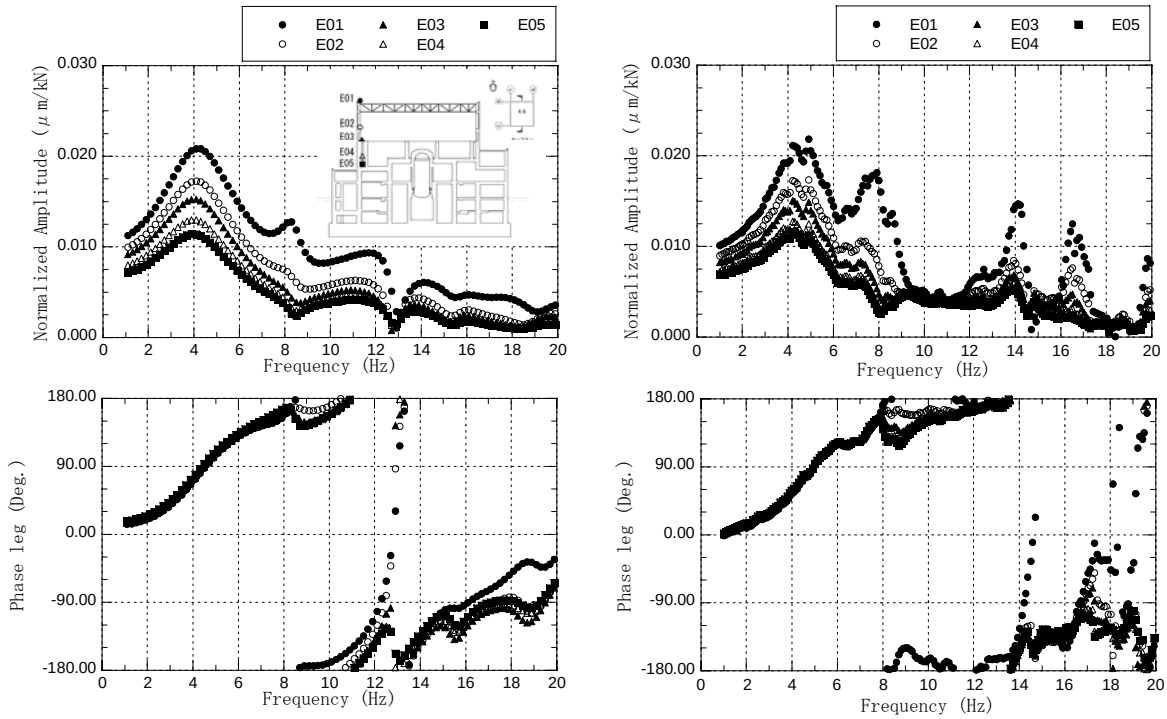

Analytical Test

Figure 7 Comparison of Simulation and Test (EW direction;RF-3F)

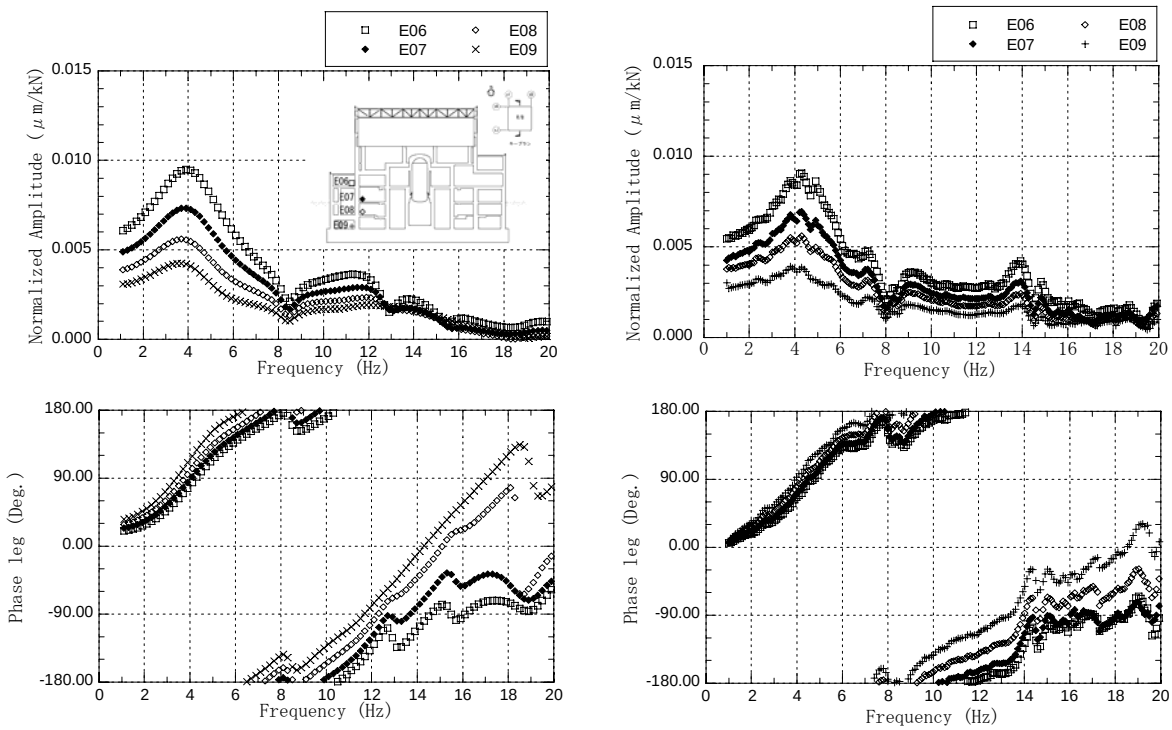

Analytical Test

Figure 8 Comparison of Simulation and Test (EW direction;2F-B2F)

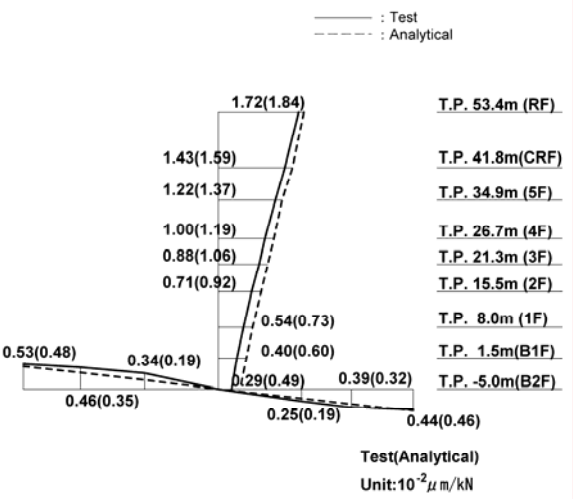

Figure 9
Comparison of 1st vibration mode (NS direction)

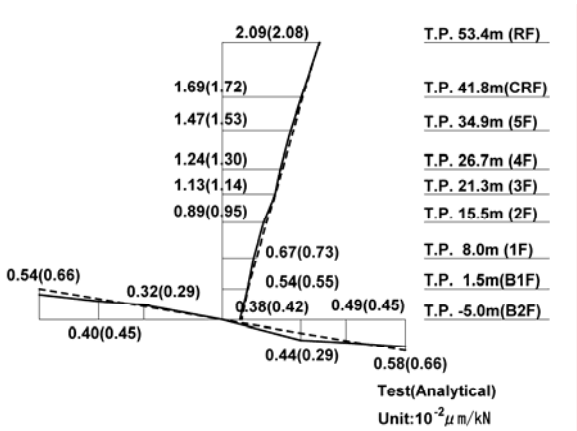

Figure 10
Comparison of 1st vibration mode (EW direction)

Table 5 Deformation Percentage(Unit:%)

		Sway	Rocking	Elastic
NS	Test	17	50	33
	Analytical	27	36	37
EW	Test	18	48	34
	Analytical	20	48	32

2.4 SIMULATION ANALYSIS WITH AN OUT-OF-PLANE DEFORMATION OF A FOUNDATION

The 6.5m thick foundation made of reinforced concrete is much thicker than OW, IW and RCCV. Therefore, it is assumed to be rigid plate in simulation analyses reported in the previous section. However, an out-of-plane deformation at a part of the foundation is slightly observed in the test result. Thus, a simulation analysis with an out-of-plane deformation of the foundation is carried out in the direction of EW where the influence with adjacent buildings is relatively small.

For the analytical model, the foundation is divided into three parts such as OW, IW,, RCCV to consider the out-of-plane deformation. Each part of the foundation is connected by the spring to evaluate the out-of-plane mode of the foundation and also soil. Figure 11 shows a soil-building analysis model with an out-of-plane deformation of a foundation.

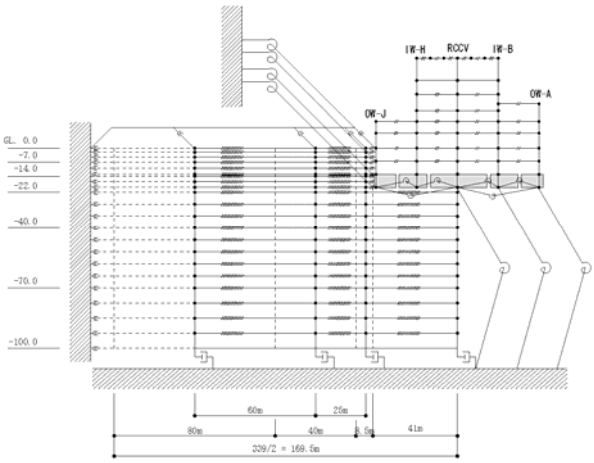

Figure 11 Simulation analysis model with an out-of-plane deformation of a foundation

The resonance curves with and without the effect are shown in Fig.12 and Fig.13. From these results, the influence with the effect is observed at the first peak and around 14Hz higher-order peak. For the first peak, the amplitude with it is slightly larger than that without it and also the peak frequency with it is

higher than that without it. In addition, the influence with it is observed around 14Hz peak caused by the excitation of IW. However, it is concluded that the influence with an out-of-plane deformation of the foundation is relatively small as an overall tendency in a resonance curve up to about 10Hz where the response of the building is dominant.

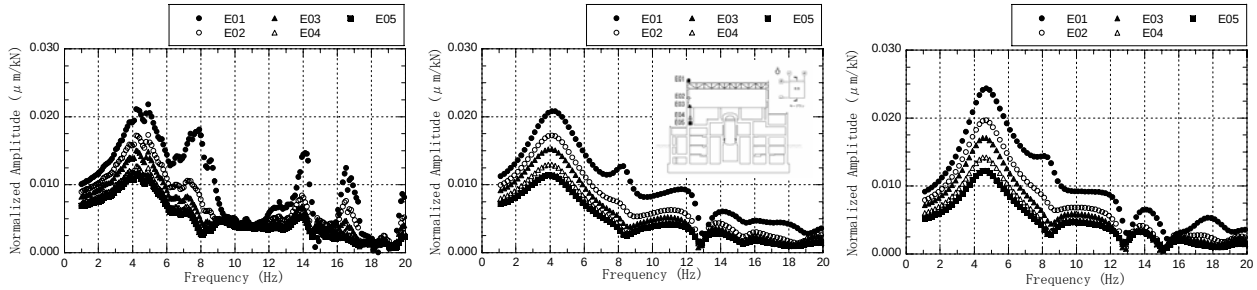

Test Not consider case Consider case

Figure 12 Resonance curves (EW direction;RF-3F)

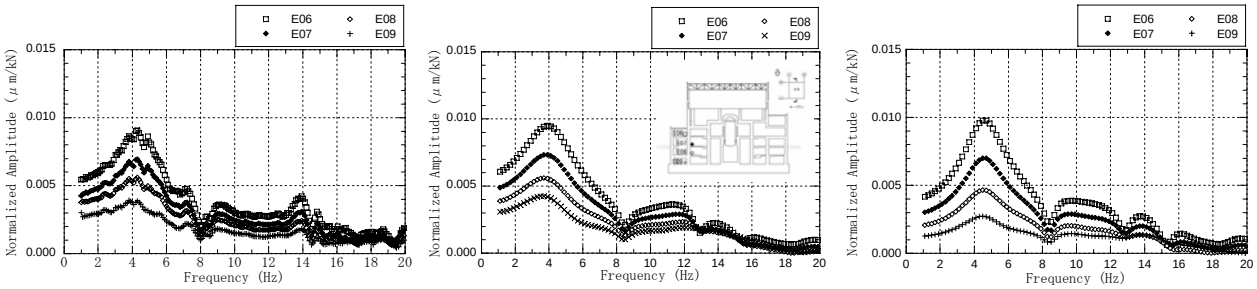

Test Not consider case Consider case

Figure 13 Resonance curves (EW direction;2F-B2F)

2.5 SIMULATION ANALYSIS WITH AN ADJACENT TURBINE BUILDING

As shown in the previous 2.3 section, the first peak's frequency of the analytical results in NS direction tends to be lower than that of the test results. In addition, a perturbation around first peak at 4.1Hz is also observed in resonance curves of test results. As one of these causes, there is an influence of the adjacent turbine building whose weight is relatively large comparing to the reactor building. Therefore, the results by simulation analysis with the adjacent turbine building in NS direction are reported in this section. Figure 14 shows the soil-building analytical model with the adjacent turbine building. The resonance curves of the analytical and test results are shown in Fig.15 and Fig.16. From these results, the influence of the adjoining turbine building appears only around first peak at about 4Hz, whose frequency of the analytical results with T/B is relatively higher than that without it and whose perturbation is also observed in the analysis with T/B. These analytical tendencies in the case with T/B are well corresponding to the test results. Therefore, to be limited in this study, it is concluded that an adjacent building influences on detailed shapes of resonance curves around the first peak that is observed in the test results.

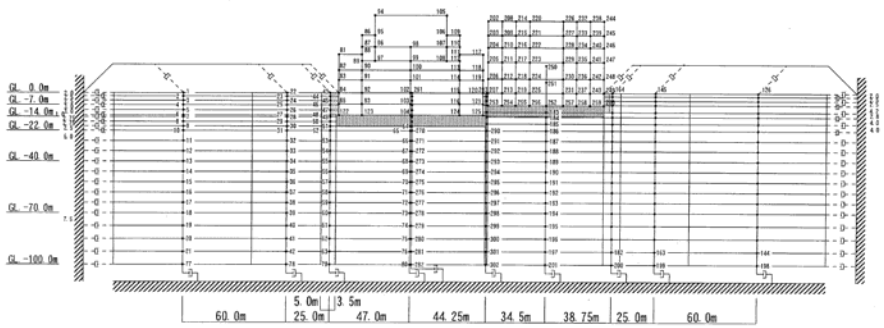

Figure 14 Simulation analysis model with the adjacent T/B

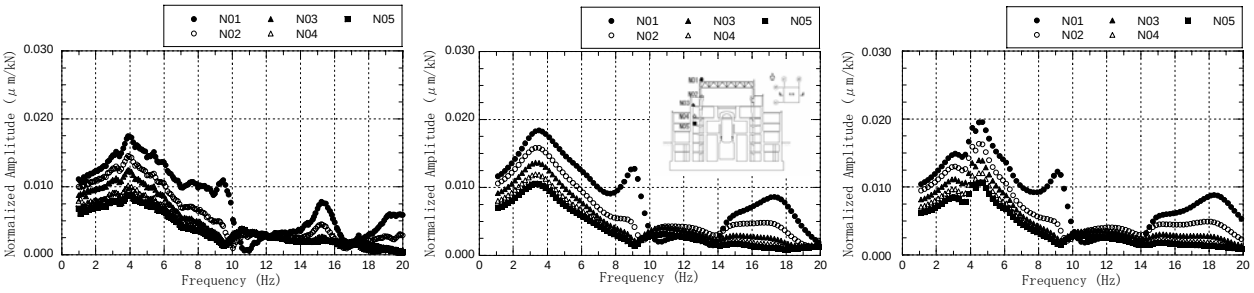

Test Not consider case Consider case

Figure 15 Resonance curves (NS direction;RF-3F)

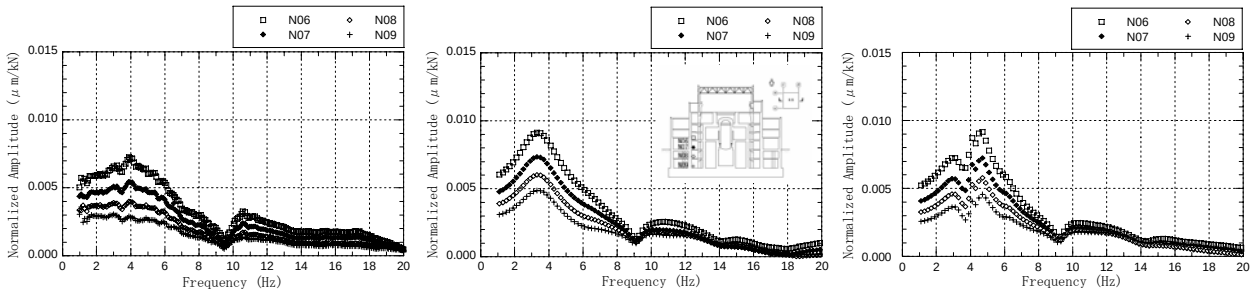

Test Not consider case Consider case

Figure 16 Resonance curves (NS direction;2F-B2F)

3. VERIFICATION FOR ASEISMIC DESIGN SAFTY

Considering the simulation analytical model shown in the previous chapter, the verification model of the building is constructed for the aseismic design safety evaluation under the basic design earthquake motion S1. Using this verification model, earthquake response analyses are carried out under S1 earthquake. Verification process for the aseismic design safety is done by comparing design seismic load with the verification model's maximum seismic response values.

3.1 RESPONSE ANALYSIS MODEL FOR VERIFICATION

So-called design model is defined as an earthquake response analysis model for design seismic load. Design seismic load is evaluated to consider an adequate margin of the response values by a design model. In addition, a design model is constructed from the conservative point of view that means the response values become large comparing to best estimate model to simulate average real situations. Based on the above background in a design model, the earthquake response analysis model in this study to verify aseismic design safety is constructed as follows:

-To consider the margin in design

-To use best estimate model for the evaluation of average real situations

This means that not all conservative ideas in a design model is removed but partially. Therefore, the verification model for aseismic design safety in Hamaoka nuclear plant is constructed as the following:

-Building model is similar to be design model.

-Viscous boundary is adopted as boundary condition of the soil model.

-Rotational spring at the bottom of the foundation is evaluated from ED method that is one of the approximation methods for the earthquake response analysis in time domain.

Properties of the soil are shown in Table 6. Properties of the backfill soil are also shown in Table 7. Soil-building analysis models for aseismic design safety evaluation are shown in Fig.17 and Fig.18. Properties of a concrete are the same as the design value as follows:

Young's Modulus : $Ec = 2.65 \times 10^7 kN/m^2$

Shear Modulus : $Gc = 1.14 \times 10^7 kN/m^2$

More detailed investigation has been studied by earthquake observation simulation analyses on Hamaoka nuclear power plant unit-4 using the verification model for aseismic design safety evaluation. Regarding this study, it will be reported in future.

3.2 SEISMIC RESPONSE RESULTS

The input earthquake motion at GL-100.0m for MDOF parallel model is calculated by using one-dimensional wave propagation theory to the basic design earthquake motion S1 defined at bedrock (GL-20.0m). Figure 19 shows the time history of acceleration and the acceleration response spectra of the input earthquake motion. For the maximum response values of the acceleration and of the shearing force under S1 earthquake, earthquake response values by the verification model are compared with design seismic load, shown in Fig.20 to Fig.23. From these results, the former is less than the latter for all members in both directions. Therefore, it is concluded that the design seismic load and aseismic design safety are verified.

Table 6 Properties of Soil

Level GL m	Density γ (kN/m^3)	Poisson's ratio ν	Shear Velocity Vs (m/s)	Shear Stiffness Go (10^{3}kN/m^2)	Stiffness degradation rate	Shear Stiffness G (10^{3}kN/m^2)	Young's Modulus E (10^{3}kN/m^2)	Damping ratio (%)
0								
-7	20	0.45	240	116	0.67	77	225	5.0
-14	20	0.44	600	721	1.00	721	2076	5.0
-22	20	0.43	680	926	1.00	926	2648	5.0
-40	20	0.42	740	1096	1.00	1096	3114	5.0
-70	20	0.41	790	1249	1.00	1249	3524	5.0
-100	20	0.40	830	1379	1.00	1379	3861	5.0
	21	0.39	910	1741	1.00	1741	4840	5.0

Table 7 Properties of Backfill Soil (Seismic response analysis)

Properties of Backfill Soil (Shear spring in the NS and the EW seismic response analysis)

Level (GL m)	Type	Density γ (kN/m^3)	Poisson's ratio ν	Shear Stiffness Go (? 0^{3}kN/m^2)	Stifness degradation rate G/Go	Shear Stiffness G (? 0^{3}kN/m^2)	Damping ratio (%)
0.0							
-2.0	Backfill Soil	20	0.45	36	0.67	25	5.0
-4.5	Backfill Soil	20	0.45	62	0.67	41	5.0
-7.0	Backfill Soil	20	0.45	79	0.67	53	5.0
-10.0	Backfill Soil	20	0.45	95	0.67	64	5.0
-13.0	Backfill Soil	20	0.45	109	0.67	73	5.0

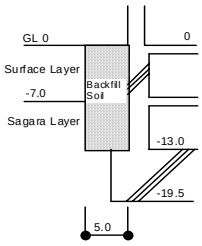

Properties of Backfill Soil (Axial spring in the NS and the EW seismic response analysis)

Level (GL m)	Type	Density γ (kN/m^3)	Poisson's ratio ν	Shear Stiffness Go (? 0^{3}kN/m^2)	Stifness degradation rate G/Go	Young扭 Modulus E (? 0^{3}kN/m^2)	Damping ratio (%)
0.0							
-1.0	Backfill Soil	20	0.45	26	0.67	51	5.0
-3.25	Backfill Soil	20	0.45	51	0.67	99	5.0
-5.75	Backfill Soil	20	0.45	72	0.67	139	5.0
-8.5	Backfill Soil	20	0.45	88	0.67	172	5.0
-11.5	Backfill Soil	20	0.45	103	0.67	200	5.0
-13.0	Backfill Soil	20	0.45	113	0.67	219	5.0

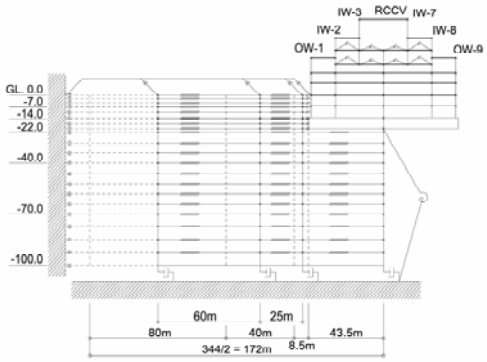

Figure 17
Seismic response analysis model (NS direction)

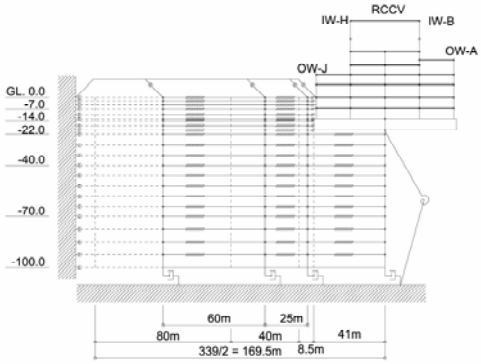

Figure 18
Seismic response analysis model (EW direction)

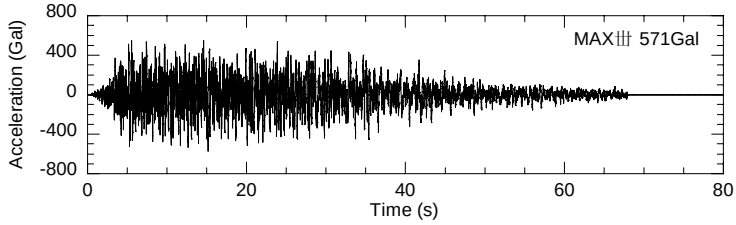

(a) Time history of input acceleration wave

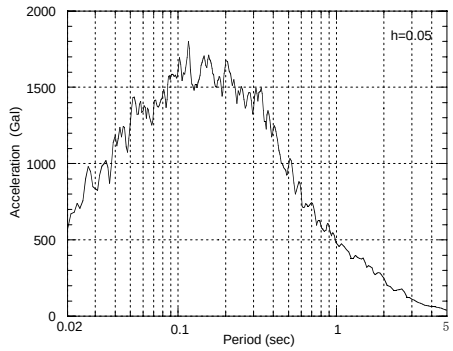

(b) Acceleration response spectra of input wave

Figure 19 Input wave

4. CONCLUSIONS

The simulation analytical results in both directions (NS and EW) are in good agreement with the test results in resonance curves.

Thus, the MDOF parallel model used in the simulation can well explain the dynamic characteristic of the real nuclear reactor building.

Moreover, the seismic response analysis using the verification model for aseismic design safety is evaluated under the basic design earthquake S1. Comparing the maximum seismic response values under S1 earthquake and the design seismic loads, the former is less than the latter for all members in both directions. Therefore, it is concluded that the design seismic load and aseismic design safety are verified.

REFERENCES

1) Onouchi, A., Tachibana, A., Niousha, A., Naito, Y., (2005), Forced vibration test of an ABWR nuclear reactor building –Data analysis and system identification-, Transactions of the 18th International Conference on Structural Mechanics in Reactor Technology (SMiRT 18) K13/3.
2) Nakagawa, S., Kuno, M., Naito, Y., Nozawa, t., Momma, T., Motohashi, S., Niwa, M., (1995) Forced vibration tests and simulation analyses of nuclear reactor building-Part1:Outline of the forced vibration tests, Transactions of the 13th International Conference on Structural Mechanics in Reactor Technology (SMiRT 13).
3) Kuno, M., Nakagawa, S., Momma, T., Mizuno, J., Naito, Y., Niwa, M., Motohashi, S., (1995) Forced vibration tests and simulation analyses of nuclear reactor building-Part2:Simulation analyses, Transactions of the 13th International Conference on Structural Mechanics in Reactor Technology (SMiRT 13).
4) Y. J. Park, C. H. Hofmayer, (1994), Technical Guidelines for Aseismic Design of Nuclear Power Plants Translation of JEAG 4601-1987.

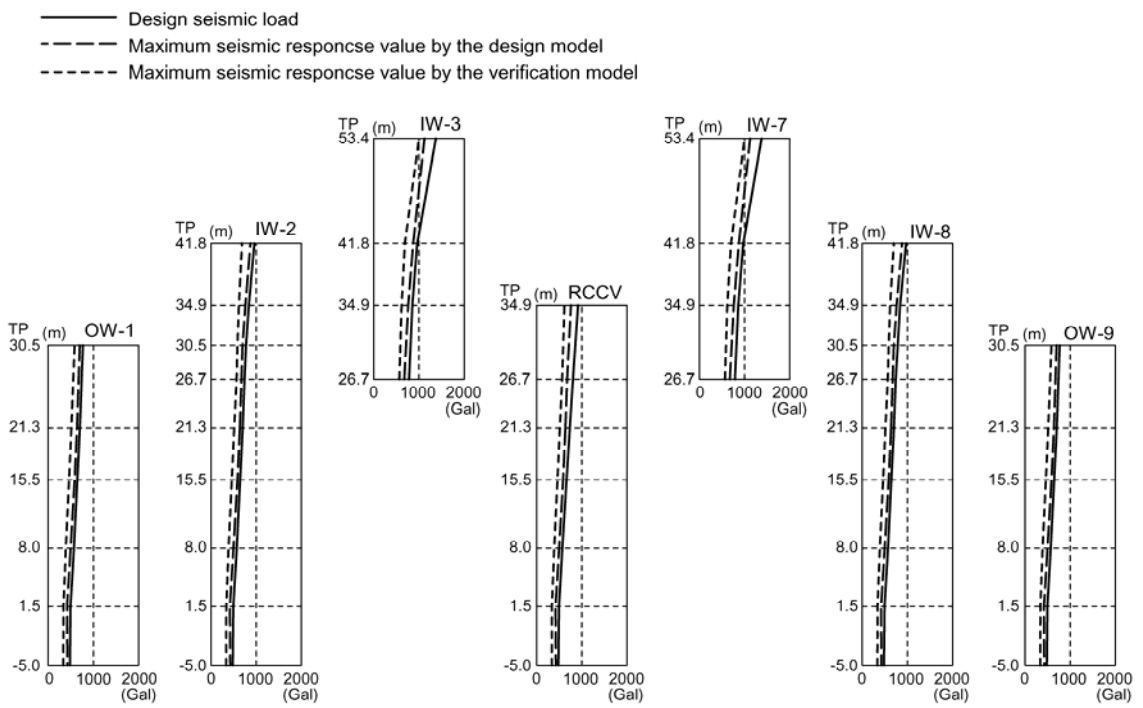

OW-1 (Gal)

Design load	Design model	Safty model
769	699	585
702	638	514
645	586	462
570	499	390
495	419	340
482	425	336

IW-2 (Gal)

Design load	Design model	Safty model
960	873	687
837	761	617
777	699	585
743	675	566
702	638	514
645	586	462
570	499	390
495	419	340
482	425	336

IW-3 (Gal)

Design load	Design model	Safty model
1374	1122	1001
960	873	687
853	761	617
782	675	566

RCCV (Gal)

Design load	Design model	Safty model
918	761	617
805	675	566
735	638	514
663	586	462
570	499	390
495	419	340
482	425	336

IW-7 (Gal)

Design load	Design model	Safty model
1376	1122	1001
970	882	699
861	761	617
787	675	566

IW-8 (Gal)

Design load	Design model	Safty model
970	882	699
837	761	617
787	699	587
743	675	566
702	638	514
645	586	462
570	499	390
495	419	340
482	425	336

OW-9 (Gal)

Design load	Design model	Safty model
769	699	587
702	638	514
645	586	462
570	499	390
495	419	340
482	425	336

Figure 20 Maximum seismic response value of the acceleration (NS direction ,The design earthquake motion S1)

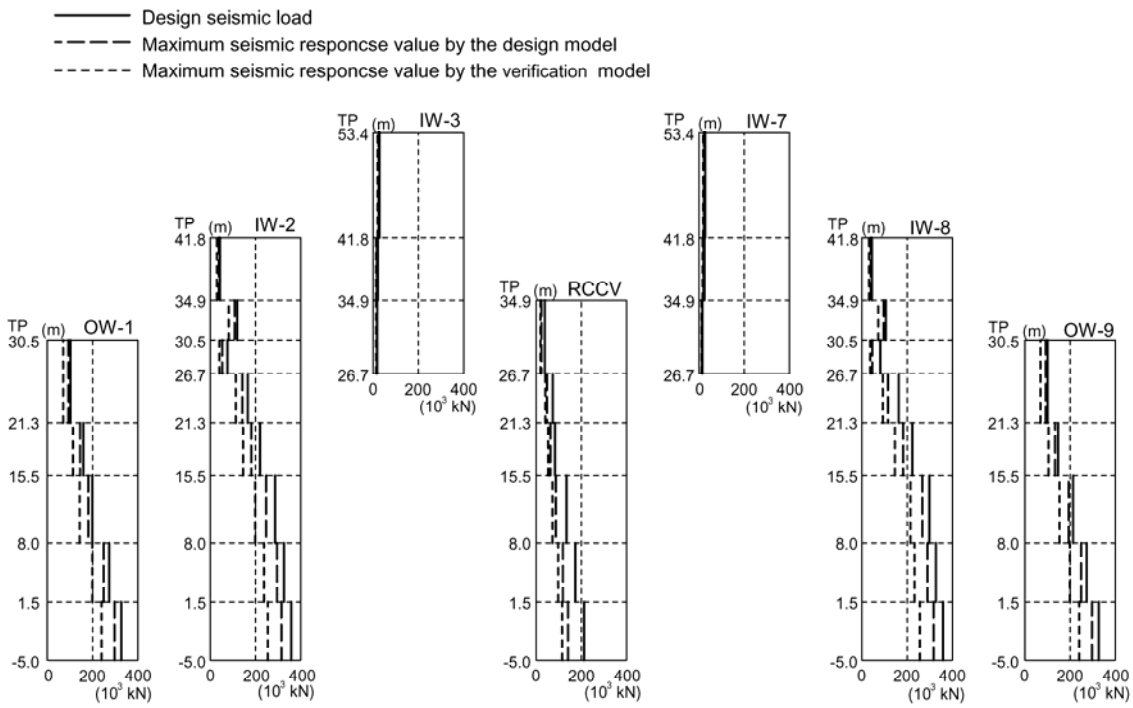

OW-1 (10^3 kN)

Design load	Design model	Safty model
102.5	93.2	70.1
159.2	144.6	113.1
199.3	181.1	143.1
273.6	248.7	199.0
326.8	297.0	239.9

IW-2 (10^3 kN)

Design load	Design model	Safty model
43.3	37.4	29.7
119.1	108.0	81.6
75.5	52.8	40.4
165.5	142.2	112.8
219.7	181.5	145.2
287.0	246.7	198.4
325.7	295.3	237.2
357.8	314.6	254.6

IW-3 (10^3 kN)

Design load	Design model	Safty model
28.2	23.8	20.1
20.4	16.6	12.8
17.8	16.2	13.2

RCCV (10^3 kN)

Design load	Design model	Safty model
38.9	23.8	19.0
73.7	47.9	40.1
83.5	63.2	53.3
134.7	87.2	72.3
173.2	118.6	97.4
212.1	141.2	115.0

IW-7 (10^3 kN)

Design load	Design model	Safty model
27.7	21.8	18.5
24.3	19.9	15.5
14.8	13.4	11.6

IW-8 (10^3 kN)

Design load	Design model	Safty model
44.5	38.9	31.0
105.6	95.8	72.3
81.2	45.5	36.6
162.8	115.1	92.3
222.8	182.0	146.0
298.5	266.5	214.2
327.2	289.2	232.3
358.6	316.5	256.1

OW-9 (10^3 kN)

Design load	Design model	Safty model
100.9	91.7	69.0
147.3	133.8	104.7
213.1	193.7	153.0
273.2	248.4	198.7
326.7	296.9	239.8

Figure 21 Maximum seismic response value of the shearing force (NS direction ,The design earthquake motion S1)

- Design seismic load
- Maximum seismic responcse value by the design model
- Maximum seismic responcse value by the verification model

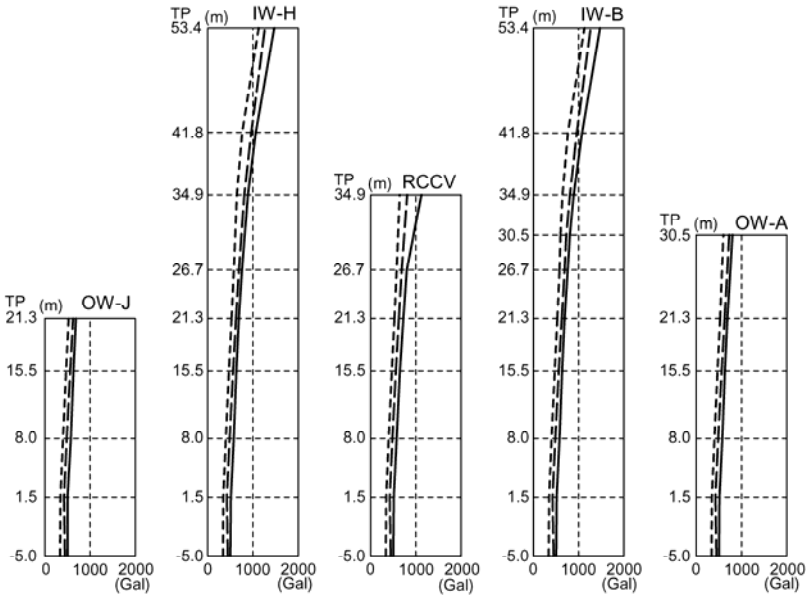

OW-J (Gal)

Design load	Design model	Safty model
688	625	527
633	560	470
576	484	401
512	423	345
502	445	338

IW-H (Gal)

Design load	Design model	Safty model
1472	1264	1126
1062	964	762
889	808	643
758	689	577
688	625	527
633	560	470
576	484	401
512	423	345
502	445	338

RCCV (Gal)

Design load	Design model	Safty model
1125	808	643
801	689	577
724	625	527
648	560	470
576	484	401
512	423	345
502	445	338

IW-B (Gal)

Design load	Design model	Safty model
1472	1264	1126
1073	957	782
889	808	643
806	727	598
758	689	577
688	625	527
633	560	470
576	484	401
512	423	345
502	445	338

OW-A (Gal)

Design load	Design model	Safty model
800	727	598
688	625	527
633	560	470
576	484	401
512	423	345
502	445	338

Figure 22 Maximum seismic response value of the acceleration (EW direction ,The design earthquake motion S1)

· Design seismic load
· Maximum seismic responcse value by the design model
· Maximum seismic responcse value by the verification model

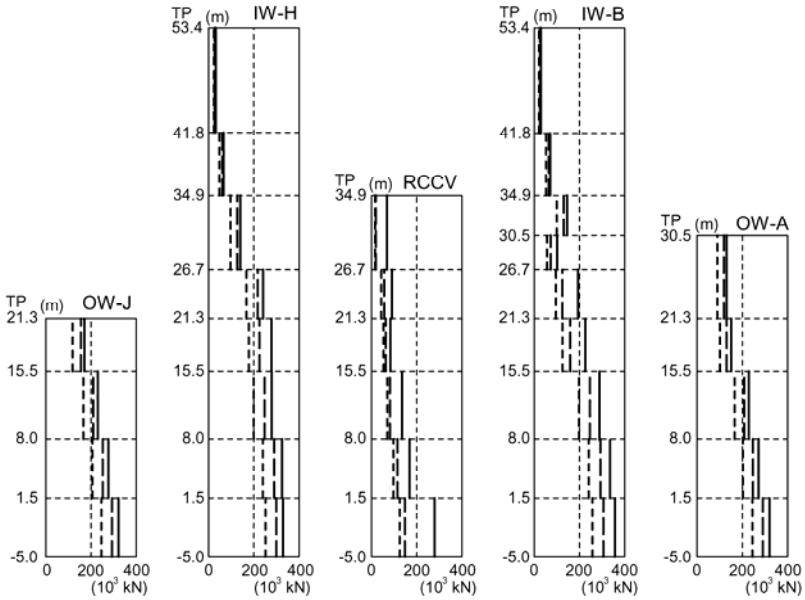

OW-J (10^3 kN)

Design load	Design model	Safty model
171.0	155.4	118.6
230.4	209.3	166.1
276.7	251.6	205.9
321.7	292.4	245.8

IW-H (10^3 kN)

Design load	Design model	Safty model
31.5	26.4	22.7
66.0	60.0	47.9
139.5	126.0	97.0
241.0	217.2	167.2
277.6	224.8	177.8
279.0	247.3	199.6
324.1	289.9	239.5
329.0	299.1	251.6

RCCV (10^3 kN)

Design load	Design model	Safty model
68.8	19.6	15.7
90.3	56.6	43.1
83.3	63.5	53.5
135.1	81.6	70.2
168.4	114.9	97.3
204.2	147.8	124.8

IW-B (10^3 kN)

Design load	Design model	Safty model
29.6	24.9	20.9
70.5	64.1	51.8
145.2	129.9	99.1
101.0	72.7	56.4
193.1	124.2	95.4
225.6	158.4	124.5
287.9	245.8	197.7
334.7	292.1	240.9
356.6	305.7	257.2

OW-A (10^3 kN)

Design load	Design model	Safty model
130.2	118.4	89.8
150.9	130.7	101.0
228.8	208.0	165.6
271.5	246.8	202.4
319.9	290.8	244.5

Figure 23 Maximum seismic response value of the shearing force (EW direction ,The design earthquake motion S1)